Externally mode-matched cavity quantum electrodynamics with charge-tunable quantum dots

Rakher, M.T.; Stoltz, N.G.; Coldren, L.A.; Petroff, P.M.; Bouwmeester, D.

Citation

Rakher, M. T., Stoltz, N. G., Coldren, L. A., Petroff, P. M., & Bouwmeester, D. (2009). Externally mode-matched cavity quantum electrodynamics with charge-tunable quantum dots. *Physical Review Letters*, *102*(9), 097403. doi:10.1103/PhysRevLett.102.097403

Externally Mode-Matched Cavity Quantum Electrodynamics with Charge-Tunable Quantum Dots

M. T. Rakher,[1,*] N. G. Stoltz,[2] L. A. Coldren,[2,3] P. M. Petroff,[2,3] and D. Bouwmeester[1,4]
[1]*Department of Physics, University of California Santa Barbara, Santa Barbara, California 93106, USA*
[2]*Materials Department, University of California Santa Barbara, Santa Barbara, California 93106, USA*
[3]*ECE Department, University of California Santa Barbara, Santa Barbara, California 93106, USA*
[4]*Huygens Laboratory, Leiden University, P.O. Box 9504, 2300 RA Leiden, the Netherlands*

(Received 3 June 2008; published 5 March 2009)

We present coherent reflection spectroscopy on a charge and dc Stark tunable quantum dot embedded in a high-quality and externally mode-matched microcavity. The addition of an exciton to a single-electron-charged quantum dot forms a trion that interacts with the microcavity just below the strong-coupling regime of cavity quantum electrodynamics. Such an integrated, monolithic system is a crucial step towards the implementation of scalable hybrid quantum-information schemes that are based on an efficient interaction between a single photon and a confined electron spin.

DOI: 10.1103/PhysRevLett.102.097403 PACS numbers: 78.67.Hc, 78.55.Cr, 78.90.+t

Hybrid quantum-information schemes combine the coherence properties and ease of manipulation of photons with the scalability and robustness of local quantum systems. Examples of local quantum systems include electron spins in quantum dots, defect centers in diamond, and trapped atoms or ions [1,2]. Hybrid schemes such as quantum repeaters and quantum networks use the coupling between the local quantum system (qubit) and the optical field to reversibly map the quantum state of a photon onto the state of the local system [3–6]. Other hybrid schemes use a joint measurement of emitted photons, which are entangled with their respective local qubit, to perform gate operations on the two spatially separated local systems [7–10]. This latter scheme can be used to create entanglement between many local qubits as needed for cluster-state quantum computation. Implementations based on trapped ions or atoms have reached operation fidelities greater than 80% for 2 remote qubit interactions. However, the overall success probabilities are currently limited to $\approx 10^{-8}$, due to the technical incompatibility of trapping the particles and coupling them efficiently to a single external optical mode [11,12]. Here we present a solid-state system that integrates a trapped, electrically controlled quantum system with near unity coupling efficiency to an external optical mode.

To achieve an efficient coupling, the quantum system must be placed in a high-quality microcavity so that it dominantly interacts with a single optical mode. Furthermore, this cavity mode must be mode matched to an external mode to ensure efficient operation at the single photon level. The ideal operating point for such hybrid schemes is deep in the weak coupling (Purcell) regime of cavity quantum electrodynamics (QED), just below the onset of strong coupling. In addition, for cluster-state and distributed quantum computation, the hybrid system must be scalable. Our system satisfies these requirements in the solid-state. It is composed of self-assembled quantum dots (QDs) (density $\approx 10\ \mu\text{m}^{-2}$) at the center of an oxidation-apertured micropillar cavity with integrated doped layers that enable an external bias to apply an electric field across the QD. This field causes carriers to tunnel in and out [13] of the QD, changing the QD charge state, and induces the quantum confined Stark effect [14], shifting the emitted photon's energy. While cavity QED has been studied using quantum dots for several years, this has been done using a neutral exciton [15,16]. Neutral excitons, bound electron-hole pairs, have been proposed as qubits [17] but seem problematic due to their quick spontaneous decay, ≈ 1 ns in GaAs, and fast dephasing [18]. The local qubit in our system is the spin of a trapped electron [19,20], which interacts with the cavity mode through the addition of an exciton, forming a short-lived trion state. Since the polarization of the emitted photon is correlated with the spin state of the remaining electron, the trion acts as a readout channel of the spin [5]. Additionally, the micropillar cavity geometry is such that the fundamental mode is a doubly degenerate $\text{HE}_{1,1}$ mode, which mode matches well to external modes due to its Gaussian-like shape [21]. Here, we report on two variations of the solid-state cavity QED system, one optimized to operate in the charge-tuning regime, and the other in the Stark-tuning regime.

The demonstration of an electrically gated QD embedded in a high Q cavity mode has become feasible through a series of scientific advances. First, the development of vertical-cavity surface-emitting lasers (VCSELs) with oxide apertures in the GaAs/AlGaAs material system enabled the creation of cavities with small mode volumes, $V_{\text{eff}} = 35(\lambda/n)^3$, while maintaining a very high Q [22]. Second, the addition of single, self-assembled InAs/GaAs QDs embedded at the axial antinode of the cavity mode provided an atomiclike emitter to couple to the optical mode [23]. Third, the use of etched trenches to define the oxidation front, as shown in Fig. 1, enabled both control over the polarization degeneracy of the cavity modes as well as global electrical connection to an array of cavities

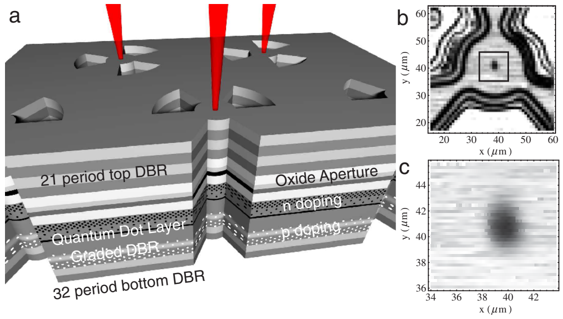

FIG. 1 (color online). (a) Schematic of the scalable cavity QED system based on electrically gated QDs embedded in oxide-apertured micropillars. (b) Two-dimensional reflectivity scan of a micropillar cavity taken with a laser resonant with the cavity mode. The mode in the center can be seen clearly as a dip in the reflected signal. (c) Higher resolution reflectivity scan taken in a 10 μm × 10 μm area containing the mode.

[24]. In the experiments presented here, the oxidation time of the aperture is such to maximize Q while minimizing the mode volume. As shown in Figs. 1(b) and 1(c), the cavity mode is to a good approximation Gaussian in lateral profile and fits to a waist of 2.2 μm, in agreement with measurements of the spacing between transverse modes [23].

Using a voltage source to drop an electric field over the QD active region is complicated by the presence of nearby material interfaces at each distributed Bragg reflector (DBR) period and at the oxide aperture region. These interfaces trap charges and result in the formation of charge domains, which reduce the field dropped across the QD region and obstruct controlled charging and Stark tuning [24]. To overcome these problems, a novel p-i-n device structure was developed in which the intrinsic region does not include the oxide aperture and the nearby p-doped $\mathrm{Al_{0.9}Ga_{0.1}As}$ DBR period is Al-content graded to and from the adjacent GaAs layers as shown in Fig. 1(a). The Al-content grading prevents the formation of triangular potential wells that arise at abrupt $\mathrm{Al_{0.9}Ga_{0.1}As/GaAs}$ interfaces. Furthermore, all doping concentrations are graded such that they are easily contacted by countersink etching without introducing unnecessary dopants near the QDs. The two variations of the solid-state cavity QED system presented here have nominally the same growth structure, but the average doping levels for the charge-tuning system are $3.5 \times 10^{18}\ \mathrm{cm^{-3}}$ ($2.5 \times 10^{18}\ \mathrm{cm^{-3}}$) for the n-doped (p-doped) layer whereas for the Stark tuning system they are $7.0 \times 10^{17}\ \mathrm{cm^{-3}}$ ($7.5 \times 10^{17}\ \mathrm{cm^{-3}}$).

To investigate the intracavity charging, we first characterized QDs outside of the cavities in the surrounding mirror region, where the Purcell effect is negligible. We monitored the photoluminescence spectrum (using a 1.25 m monochromator coupled with a CCD array) under 150 fs, 860 nm Ti:sapphire laser excitation with 50 nW average power as the applied bias is varied. A typical trace for a single QD is shown in Fig. 2(a). Near 18 V applied bias, the QD emission abruptly changes 6 meV to lower energy. This is the characteristic energy separation for the transition between the neutral exciton, X^0, and the singly electron-charged exciton, X^- [13,25]. To verify the charge designations as X^0 and X^-, we also measured the time-resolved decay of the photoluminescence. The result is shown in Fig. 2(b), with curves taken at biases below (above) 18 V labeled as dashed (straight). Because of the presence of optically dark states, the X^0 decay traces have a distinctive biexponential behavior, whereas the X^- decay are single exponentials [24,26].

The same lifetime measurement is performed for QDs in the cavity region which are on resonance with a polarization-degenerate fundamental mode as shown in Fig. 2(c) (this was possible for approximately 10% of cavities), and the results qualitatively replicate that of the bulk QDs. However, the effect of the high Q cavity strongly reduces the emission lifetime by the Purcell effect. For some X^- cases, this lifetime approaches 150 ps, the timing resolution of our experiment. Nonetheless, a deconvolved lifetime of 137 ± 21 ps was obtained for the fastest X^- transition and 321 ± 15 ps for the X^0. This yields a Purcell enhancement, $F_p = \tau_o/\tau_{\mathrm{cav}}$, of approximately 7 for the X^-. We measure that on average ($F_p = 2.8 \pm 0.22$ for 4 X^0 transitions and 5.9 ± 0.96 for 6 X^-) the Purcell enhancement is stronger for X^- than for X^0. Because both transitions have similar lifetimes in the DBR region, resulting from similar oscillator strengths, one would expect both to have similar Purcell effects. However, this is not found experimentally and may be due to a better matching of the transition dipole moment to the cavity mode polar-

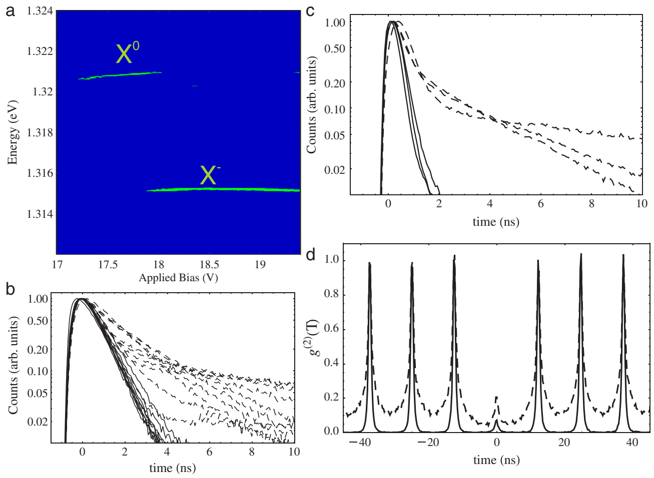

FIG. 2 (color online). (a) Photoluminescence spectra as a function of applied bias for a QD in the mirror region at 4 K. (b) Emission decay traces for 10 QDs in the mirror region. Straight traces are taken with 18.5 V applied bias (X^-) and dashed traces are taken with 17.5 V applied bias (X^0). (c) Emission decay traces for QDs on resonance with cavity modes for several different cavities. The straight (dashed) traces correspond to an X^- (X^0) decay. (d) $g^{(2)}(\tau)$ measurements for an X^- (straight) and X^0 (dashed) transition.

ization for the X^-. This could be explained by theoretical calculations beyond the standard techniques for calculating the optical transitions of a QD [27]. In addition, the second-order photon correlation function, $g^{(2)}(\tau)$, was measured as shown in Fig. 2(d) for an X^0 and an X^- transition. While both clearly demonstrate single photon behavior, the X^- is much cleaner due to its fast, single exponential decay. The measured single photon ($g^{(2)}(0) < 0.25$) count rate was typically 3×10^6 s^{-1} for an X^- with an 80 MHz pump rate, yielding a 25% extraction efficiency for the QD when corrected for the optical and detection losses of the setup (15%).

While the lifetime measurements indicate that the emission is coupled to the cavity mode, it does not yield a quantitative measure of the coupling strength, g, or the mode-matching efficiency. To do this, one must probe the coupled system coherently and we accomplish this by measuring the reflectivity of the cavity-QD system [15,16]. The reflection spectrum can be derived from the Jaynes-Cummings Hamiltonian using the input-output formalism and under sufficiently weak probing of a symmetric cavity [28–31], can be expressed as

$$R(\omega) = \left| 1 - \frac{\kappa[\gamma - i(\omega - \omega_{\mathrm{QD}})]}{[\gamma - i(\omega - \omega_{\mathrm{QD}})][\kappa - i(\omega - \omega_c)] + g^2} \right|^2, \tag{1}$$

where g is the emitter-cavity coupling, ω_{QD} (ω_c) is the emitter (cavity) resonance, γ is the dipole decay rate, and κ is cavity field decay rate. If there are no QDs coupled to the cavity mode, the spectrum shows a single dip at the cavity resonance with a width equal to the cavity field decay rate, κ, as shown in Fig. 3(a). For this micropillar, a fit to the data yields $\kappa = 24.1$ μeV, corresponding to $Q = 27\,000$. The depth of this dip is a measure of how well the probe beam is mode matched to the cavity, and in this case the coupling efficiency is greater than 96%. This remarkably high efficiency implies that reliable information transfer at the single photon level is feasible and would constitute an increase in the success probability of a two-photon experiment [11,12] by 3–4 orders of magnitude. If a QD is coupled to the microcavity, the reflection spectrum is drastically altered. Figure 3(b) shows the absolute reflection spectrum of the cavity mode interacting with a single QD transition. By fitting this spectrum to Eq. (1), we obtain an emitter-cavity coupling of $g = 9.7$ μeV and a dipole decay rate of $\gamma = 1.9$ μeV. Since $g/\kappa = 0.402$, the emitter-cavity system is deep in the Purcell (weak-coupling) regime and at the precipice of strong-coupling, $g/\kappa > 0.5$, exactly in the region ideally suited for hybrid quantum-information schemes [5,6,8,9]. The spectrum, with resolution limited by the probe laser linewidth, completely characterizes the system. Additionally, it reveals the natural linewidth of the QD transition with a signal much greater than achieved in transmission or differential transmission. In conclusion, the combination of these results for the cavity QED system in the charge-tuning regime demonstrates that it is ideal for hybrid quantum-information processing.

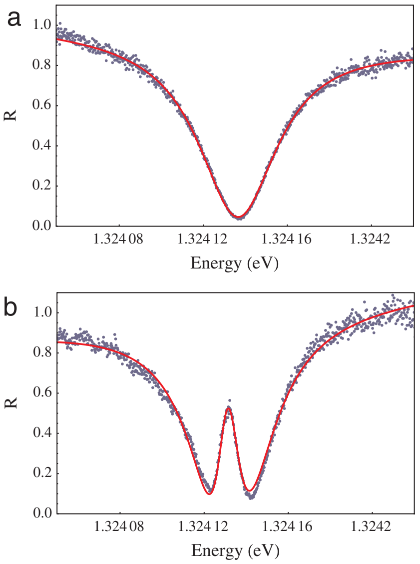

FIG. 3 (color online). (a) Cavity reflection spectrum of an unloaded micropillar cavity measured by recording the reflected signal of a tunable-wavelength laser. Equation (1) with $g = 0$ plus a linear background is used to fit the data. (b) Cavity reflection spectrum of a QD coupled to the micropillar cavity in (a). Eq. (1) plus a linear background is used to fit the data.

We now turn to the Stark-tuning cavity QED system. Since the coupling between the QD and the cavity mode depends on the spectral detuning, an external control is necessary to reach resonance. In QD systems without electrical gating, this control is achieved by adjusting the sample temperature [16]. However, this control typically decreases coherence through higher phonon occupations and is not scalable. An applied electric field can also tune the QD transition via the Stark effect without the negative effects of temperature and in principle can be scalable by gating each cavity separately. In order to illustrate this effect and potential applications, we utilized a polarization nondegenerate cavity mode. As mentioned in Ref. [24], an engineered ellipticity of the aperture lifts the polarization degeneracy, creating two orthogonal linear polarization modes (denoted as H and V) as illustrated in Fig. 4(a). Because the Q factor is very high (40 000), the modes can be spectrally separated by as little as 50 μeV and still be resolved. This enables the quantum dot transition to be Stark-shift tuned into resonance with two modes as shown in Fig. 4(b). Note that the dependence is nonlinear with bias as expected for the quantum confined Stark effect [14].

By Stark-shift tuning the QD emission, the Purcell effect is observed on resonance with each mode. Stark-shift tuning as opposed to current induced heating was confirmed by observing a constant QD linewidth over the tuning range. For several applied biases, the QD emission decay curve is measured, see Fig. 4(c), and the extracted lifetime is plotted as a function of spectral position as shown in

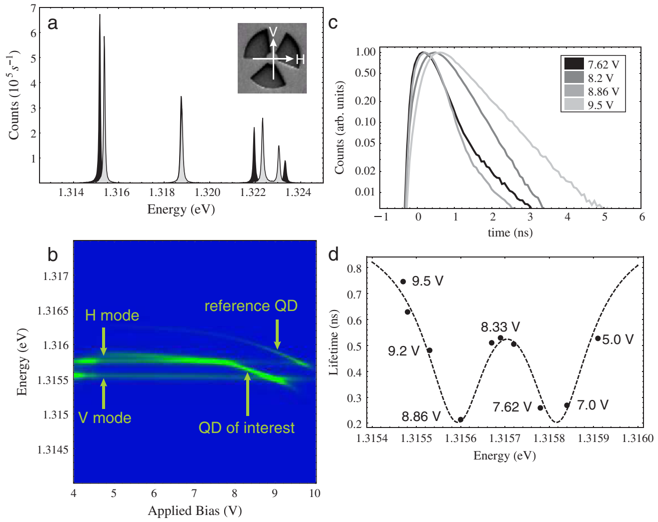

FIG. 4 (color online). (a) Microphotoluminescence spectra of nondegenerate optical modes in a micropillar. H (V) polarized modes are black (grey). Inset: SEM image of a micropillar. (b) Photoluminescence spectra as a function of applied bias for two QDs (labeled QD of interest and reference QD) and two nondegenerate fundamental cavity modes (labeled H mode and V mode). (c) Lifetime traces for a few bias settings; 7.62, 8.2, 8.86, and 9.5 V. (d) Deconvolved lifetimes as a function of emission energy with fit.

Fig. 4(d). The dips in the transition lifetimes measured on resonance are a clear consequence of the Purcell effect. The lifetimes at the resonance of each mode is measured to be 220 ps as shown in Fig. 4(d), approximately 5 times shorter than the bulk lifetime. The appearance of a biexponential, most prevalent for the on resonance biases, in Fig. 4(c) is attributed to a small fraction (~4%) of photons collected from QDs outside the mode volume. Stark-shift tuning when used in addition to charge tuning constitutes a completely bias-controlled, solid-state cavity QED system.

In conclusion, we presented a solid-state cavity QED system which has near ideal properties for photon electron-spin coupling as needed for hybrid quantum-information processing. The unique features of our system are intracavity electron charging, near perfect mode matching, polarization control of the cavity modes, and operation deep in the Purcell regime. In addition, the cavity-QD coupling can be controlled via the Stark effect, which has applications for quantum and classical communication. The combination of this work with spin initialization, manipulation, and readout [25,32,33] as well as techniques for active positioning of quantum dots [34] will bring the implementation of solid-state hybrid quantum-information protocols within reach.

The authors would like to thank M. P. Van Exter and W. Yao for useful discussions. This work was supported by NSF NIRT No. 0304678, DARPA No. MDA 972-01-1-0027, and Marie-Curie EXT-CT-2006-042580.

*mrakher@nist.gov
Present address: National Institute of Standards and Technology, Gaithersburg, MD 20899, USA.

[1] J. M. Raimond, M. Brune, and S. Haroche, Rev. Mod. Phys. **73**, 565 (2001).
[2] H. Mabuchi and A. C. Doherty, Science **298**, 1372 (2002).
[3] S. J. van Enk, J. I. Cirac, and P. Zoller, Phys. Rev. Lett. **78**, 4293 (1997).
[4] J. I. Cirac, P. Zoller, H. J. Kimble, and H. Mabuchi, Phys. Rev. Lett. **78**, 3221 (1997).
[5] W. Yao, R. Liu, and L. J. Sham, Phys. Rev. Lett. **92**, 217402 (2004).
[6] W. Yao, R. B. Liu, and L. J. Sham, Phys. Rev. Lett. **95**, 030504 (2005).
[7] R. Raussendorf and H. J. Briegel, Phys. Rev. Lett. **86**, 5188 (2001).
[8] Y. L. Lim, A. Beige, and L. C. Kwek, Phys. Rev. Lett. **95**, 030505 (2005).
[9] S. D. Barrett and P. Kok, Phys. Rev. A **71**, 060310(R) (2005).
[10] C. Simon *et al.*, Phys. Rev. B **75**, 081302(R) (2007).
[11] D. L. Moehring *et al.*, Nature (London) **449**, 68 (2007).
[12] W. Rosenfeld, S. Berner, J. Volz, M. Weber, and H. Weinfurter, Phys. Rev. Lett. **98**, 050504 (2007).
[13] R. J. Warburton *et al.*, Nature (London) **405**, 926 (2000).
[14] P. W. Fry *et al.*, Phys. Rev. Lett. **84**, 733 (2000).
[15] K. Srinivasan and O. Painter, Nature (London) **450**, 862 (2007).
[16] D. Englund *et al.*, Nature (London) **450**, 857 (2007).
[17] P. Chen, C. Piermarocchi, and L. J. Sham, Phys. Rev. Lett. **87**, 067401 (2001).
[18] C. Kammerer *et al.*, Appl. Phys. Lett. **81**, 2737 (2002).
[19] A. V. Khaetskii, D. Loss, and L. Glazman, Phys. Rev. Lett. **88**, 186802 (2002).
[20] I. A. Merkulov, A. L. Efros, and M. Rosen, Phys. Rev. B **65**, 205309 (2002).
[21] M. Pelton *et al.*, IEEE J. Quantum Electron. **38**, 170 (2002).
[22] C. Wilmsen, H. Temkin, and L. A. Coldren, *Vertical-Cavity Surface-Emitting Lasers* (Cambridge University Press, Cambridge, England, 1999).
[23] N. G. Stoltz *et al.*, Appl. Phys. Lett. **87**, 031105 (2005).
[24] S. Strauf *et al.*, Nat. Photon. **1**, 704 (2007).
[25] M. Atature *et al.*, Science **312**, 551 (2006).
[26] J. M. Smith *et al.*, Phys. Rev. Lett. **94**, 197402 (2005).
[27] G. A. Narvaez, G. Bester, and A. Zunger, Phys. Rev. B **72**, 245318 (2005).
[28] J. T. Shen and S. Fan, Opt. Lett. **30**, 2001 (2005).
[29] E. Waks and J. Vuckovic, Phys. Rev. Lett. **96**, 153601 (2006).
[30] E. Waks and J. Vuckovic, Phys. Rev. A **73**, 041803(R) (2006).
[31] A. Auffèves-Garnier, C. Simon, J.-M. Gérard, and J.-P. Poizat, Phys. Rev. A **75**, 053823 (2007).
[32] B. D. Gerardot *et al.*, Nature (London) **451**, 441 (2008).
[33] M. H. Mikkelsen *et al.*, Nature Phys. **3**, 770 (2007).
[34] K. Hennessy *et al.*, Nature (London) **445**, 896 (2007).